Journal of Power Sources 248 (2014) 205–211

Contents lists available at ScienceDirect

Journal of Power Sources

journal homepage: www.elsevier.com/locate/jpowsour

Short communication

Copper nitrate hydrate as novel high capacity anode material for lithium-ion batteries

Kaiqiang Wu, Dongjie Wang, Lianyi Shao, Miao Shui, Rui Ma, Mengmeng Lao, Nengbing Long, Yuanlong Ren, Jie Shu*

Faculty of Materials Science and Chemical Engineering, Ningbo University, Ningbo 315211, Zhejiang Province, People's Republic of China

HIGHLIGHTS

- For the first time, $Cu(NO_3)_2{\cdot}xH_2O$ is studied as a novel lithium storage anode material.
- $Cu(NO_3)_2{\cdot}xH_2O$ exhibits an initial discharge capacity of about 2200 mAh g^{-1}.
- $Cu(NO_3)_2{\cdot}xH_2O$ obtained at 160 °C delivers a reversible capacity of 597.6 mAh g^{-1} after 30 cycles.

GRAPHICAL ABSTRACT

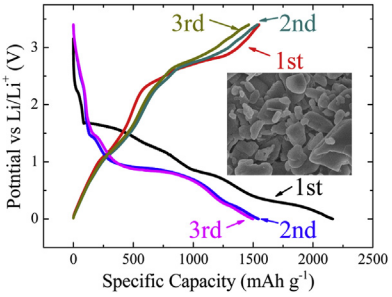

ARTICLE INFO

Article history:
Received 2 August 2013
Received in revised form
16 September 2013
Accepted 19 September 2013
Available online 30 September 2013

Keywords:
Lithium-ion batteries
Copper nitrate hydrate
Anode material
Heat-treatment

ABSTRACT

For the first time, $Cu(NO_3)_2{\cdot}xH_2O$ ($x \leq 2.5$) is investigated as a new lithium storage anode material for lithium-ion batteries. The impressive characteristic of $Cu(NO_3)_2{\cdot}xH_2O$($x \leq 2.5$)/Li cell is the high initial discharge capacity reaching to around 2200 mAh g^{-1}. To make a comparison, $Cu(NO_3)_2{\cdot}2.5H_2O$ electrodes are used as raw materials and heat-treated at 80, 120 and 160 °C. Among all the three samples, $Cu(NO_3)_2{\cdot}xH_2O$ ($x < 2.5$) obtained at 160 °C shows the highest reversible capacity of 597.6 mAh g^{-1} and the best cycling stability after 30 cycles. The difference in electrochemical behaviors is attributed to the variation of surface morphology, crystal water and particles size after heat-treatment at different temperatures. Besides, the thermal reaction results also show that $Cu(NO_3)_2{\cdot}xH_2O$ ($x < 2.5$) obtained at 160 °C has the highest thermal stability among all the three samples after repeated cycles. The present findings can provide the fact that $Cu(NO_3)_2{\cdot}xH_2O$ (≤ 2.5) may be a promising anode material for lithium-ion batteries.

© 2013 Elsevier B.V. All rights reserved.

1. Introduction

It is well known that transition metal oxides express the advantages of higher specific capacity, better electrochemical stability and more excellent cycle retention than conventional carbonaceous materials [1–3]. Among different kinds of transition metal oxides, CuO attracted more attentions because of its high theoretic specific capacity of 670 mAh g^{-1}. Moreover, it is generally accepted that different morphologies of CuO, such as nanoflower [2], hollow dandelion-like spheres [4] and leaf-shaped [5], show different electrochemical performances as anodes in lithium-ion batteries. However, those transition metal oxides suffer from severe drawbacks, such as poor electronic conductivity and huge polarization in lithium-ion batteries, which are the main hindrances to their commercial use. Due to these limitations, it seems necessary to turn the efforts towards complex transition metal oxides [6–8] or synthesis of transition metal oxides/carbon composites [9–11] to improve the electrochemical properties.

* Corresponding author. Tel.: +86 574 87600787; fax: +86 574 87609987.
E-mail addresses: sergio_shu@hotmail.com, shujie@nbu.edu.cn (J. Shu).

0378-7753/$ – see front matter © 2013 Elsevier B.V. All rights reserved.
http://dx.doi.org/10.1016/j.jpowsour.2013.09.079

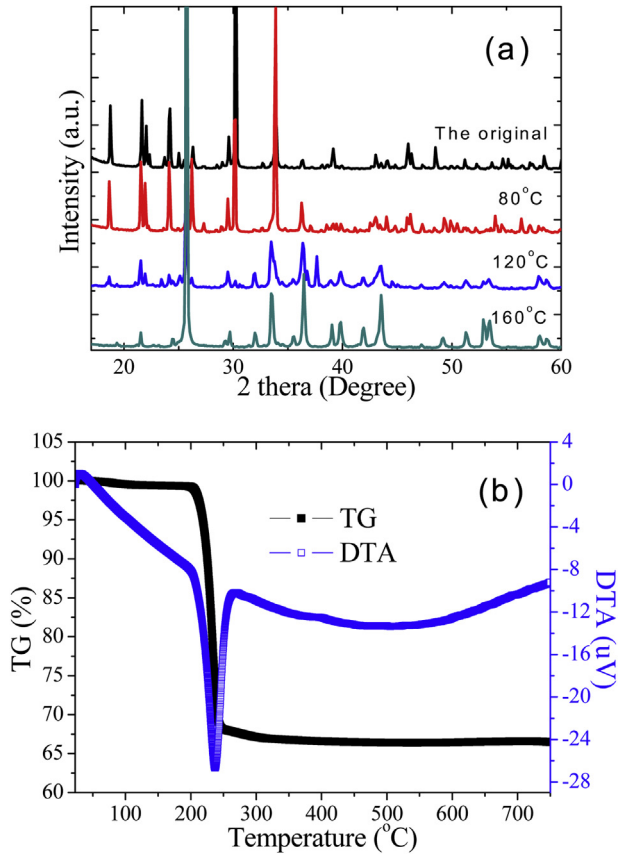

Fig. 1. (a) XRD patterns of $Cu(NO_3)_2{\cdot}xH_2O$ ($x \leq 2.5$) samples obtained at different heat-treatment temperatures and (b) TG-DTA curves of $Cu(NO_3)_2{\cdot}2.5H_2O$ in argon.

Most recently, many transition metal nitrides have been widely studied as anode materials due to their high reversibility, large reversible capacity and satisfactory stability [12–14]. As reported [12], Cu_3N exhibited good cycle life and excellent rate capability as a candidate anode material. Meanwhile, the reaction mechanism of Ge_3N_4 [13] with lithium was investigated as well. It exhibits high capacity of 500 mAh g^{-1}. Moreover, ternary lithium transition metal nitrides, such as Li_3FeN_2 [15] and Li_7MnN_4 [16], have been introduced in the last two decades, which show good cycle stability and high specific capacity. However, those ternary lithium transition metal nitrides undergo the drawback of moisture sensitivity before being treated as electrode materials in lithium-ion batteries.

Till now, no report about nitrates as lithium storage materials has been reported in the past decades. In the present work, copper nitrate hydrate is studied as a novel high capacity anode material for lithium-ion batteries, and its electrochemical properties and physical characterizations are examined.

2. Experimental

$Cu(NO_3)_2{\cdot}2.5H_2O$ (Aladdin Chemistry) was purchased with analytical grade and used as received without further purification. The slurry for working electrode was composed of $Cu(NO_3)_2{\cdot}2.5H_2O$, carbon black, and polyvinylidene fluoride as a binder with a composition of 4:1:1 in *N*-methyl pyrrolidinone solvent. Then the slurry was coated on Cu-foil collector as working electrode and treat-treated at 80, 120 and 160 °C in vacuum for 12 h.

The electrochemical cells were composed of copper nitrate hydrate electrode as working electrode, metallic lithium foils as reference and counter electrodes, 1 M $LiPF_6$ dissolved in ethylene carbonate–dimethyl carbonate (1:1 in volume) as electrolyte, and Whatman glass fiber as separator. The simulated cells were assembled in an argon-filled glove box. The patterns for microstructure were measured by Bruker AXS D8 Focus X-ray diffraction (XRD) instrument. The surface morphologies were observed by Hitachi S3400 scanning electron microscopy (SEM). Electrochemical characteristics of the cells were recorded by multi-channel Land battery test system. Electrochemical impedance spectroscopy (EIS) analysis was carried out by CHI 660D electrochemical workstation with the frequency range of 10^5–10^{-2} Hz. Thermogravimetric (TG) and differential thermal analysis (DTA) behaviors of the original and lithiated samples were investigated by a Seiko TG/DTA 6300 apparatus with a heating rate of 10 °C min^{-1} in the temperature range from 23 to 800 °C under argon atmosphere.

3. Results and discussion

Fig. 1a shows the XRD patterns of copper nitrate hydrate heat-treated at different temperatures. As seen from Fig. 1a, it is clear that the seven strongest peaks at 18.82, 21.56, 21.99, 24.18, 29.64, 30.29 and 33.90° are in good agreement with the (110), (−211), (211), (−204), (114), (−404) and (314) lines in the JCPDS card No. 75-1493 representing the compound of $Cu(NO_3)_2{\cdot}2.5H_2O$. The cell parameters of $Cu(NO_3)_2{\cdot}2.5H_2O$ are a = 16.45 Å, b = 4.941 Å, c = 15.96 Å and β = 93.750° with a space group of 12/a. Fig. 1a also shows the XRD patterns of copper nitrate hydrate obtained at 80, 120 and 160 °C, which are similar to the original pattern before heat-treatment, except for the change of relative intensity. No impurity, such as CuO and Cu_3N, can be observed in Fig. 1a.

The typical TG-DTA curves of commercial $Cu(NO_3)_2{\cdot}2.5H_2O$ are characterized in the argon atmosphere as shown in Fig. 1b. The obtained profile clearly indicates that the decomposition process of $Cu(NO_3)_2{\cdot}2.5H_2O$ proceeds in several steps. It can be observed that a slight weight loss of 0.7% appears between 23 and 200 °C, which is contributed to the evaporation of absorbed water and the partial loss of crystallized water. An abrupt weight loss of 31.3% occurs between 200 and 250 °C from the TG curves, assigning to the total loss of crystallized water and the following decomposition of $Cu(NO_3)_2$ powders into CuO and gaseous products. These decomposition steps are in accordance with those suggested by I.V. Morozov [17] and can be expressed by following equations:

$$Cu(NO_3)_2{\cdot}2.5H_2O \rightarrow Cu(NO_3)_2{\cdot}H_2O + 1.5H_2O\uparrow \quad (1)$$

$$Cu(NO_3)_2{\cdot}H_2O \rightarrow Cu(NO_3)_2 + H_2O\uparrow \quad (2)$$

$$2Cu(NO_3)_2 \rightarrow 2CuO + 4NO_2\uparrow + O_2\uparrow \quad (3)$$

Based on the above decomposition process and XRD results, it is clear that $Cu(NO_3)_2{\cdot}2.5H_2O$ may lose different amounts of crystallized water after heat-treatment at different temperatures (80, 120 and 160 °C). Therefore, the sample heat-treated at different temperatures should be defined as $Cu(NO_3)_2{\cdot}2.5H_2O$ for 80 °C and $Cu(NO_3)_2{\cdot}xH_2O$ ($x < 2.5$) for 120 and 160 °C.

Fig. 2a–f compares the surface morphologies of $Cu(NO_3)_2{\cdot}xH_2O$ ($x \leq 2.5$) samples obtained at 80, 120 and 160 °C. It is clear that distinct difference in the practice size appears due to different heat-treatment temperatures. After a heat-treatment at 80 °C, the sample shows the aggregation of many rod-like particles into bigger secondary particles. The size of rod-like particles ranges from 2.0 to 4.0 μm as observed in Fig. 2a and b. Furthermore, a layer of film-like substance is covering on the surface of samples which makes the formation of larger bulk secondary particles. The

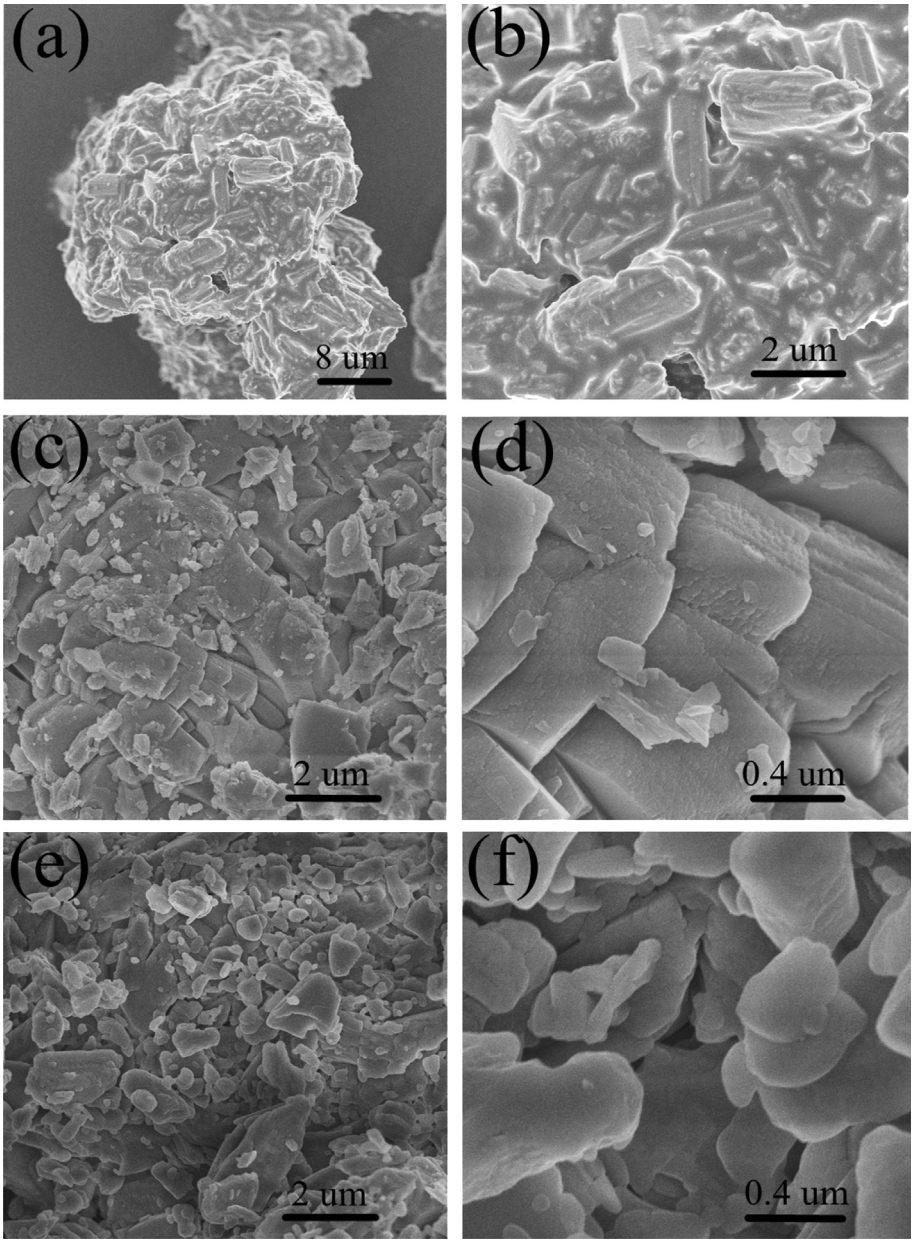

Fig. 2. SEM images of $Cu(NO_3)_2{\cdot}xH_2O$ ($x \leq 2.5$) samples obtained at different heat-treatment temperatures. (a, b) 80 °C; (c, d) 120 °C; (e, f) 160 °C.

continuous film disappears after the heat-treatment temperature increasing to 120 °C, and many cracks appear on the rough surface of the huge secondary particles as shown in Fig. 2c and d. Compared to the materials heat-treated at 80 and 120 °C, the sample heat-treated at 160 °C becomes smaller irregular particle sizes (0.1–0.8 μm) as shown in Fig. 2e and f. It suggests that $Cu(NO_3)_2{\cdot}xH_2O$ ($x \leq 2.5$) shows cracks at 120 °C and breaks into irregular bulks at 160 °C. As a result, the sample obtained at 160 °C shows larger specific surface area for Li^+ ions diffusion than that of the materials heat-treated at 80 and 120 °C.

The initial three discharge–charge curves for $Cu(NO_3)_2{\cdot}xH_2O$ ($x \leq 2.5$) samples obtained at 80, 120 and 160 °C between 0.0 and 3.4 V are shown in Fig. 3. For $Cu(NO_3)_2{\cdot}2.5H_2O$ prepared at 80 °C, three potential plateaus are observed at 1.6, 0.8 and 0.4 V during the first discharge process as shown in Fig. 3a. These potential plateaus are similar with those delivered by samples heat-treated at 120 and 160 °C as shown in Fig. 3c and e. However, $Cu(NO_3)_2{\cdot}xH_2O$ ($x < 2.5$) prepared at 160 °C displays another short potential plateau at 1.3 V, which is probably attributed to the effect of absorbed/crystallized water and surface morphology on the electrochemical reactions between $Cu(NO_3)_2{\cdot}xH_2O$ ($x < 2.5$) and Li during the discharge process. Besides, different solid electrolyte interface (SEI) film formed in the initial discharge and different electrochemical polarization also lead to the variation of potential plateaus. In the following discharge process, there is a long potential plateau remaining at 0.8 V for all the three samples.

For the delithiation process, $Cu(NO_3)_2{\cdot}2.5H_2O$ prepared at 80 °C exhibiting a long potential plateau at 2.8 V, which is different with those displayed by $Cu(NO_3)_2{\cdot}xH_2O$ ($x < 2.5$) obtained at 120 and 160 °C. As the temperature increase, the charge curves for $Cu(NO_3)_2{\cdot}xH_2O$ ($x < 2.5$) prepared at 120 and 160 °C show several additional short delithiated plateaus, which appear at 2.6 and 2.9 V in Fig. 3c, and 2.4 and 2.8 V in Fig. 3e. These differences can be attributed to the different surface morphologies and absorbed/

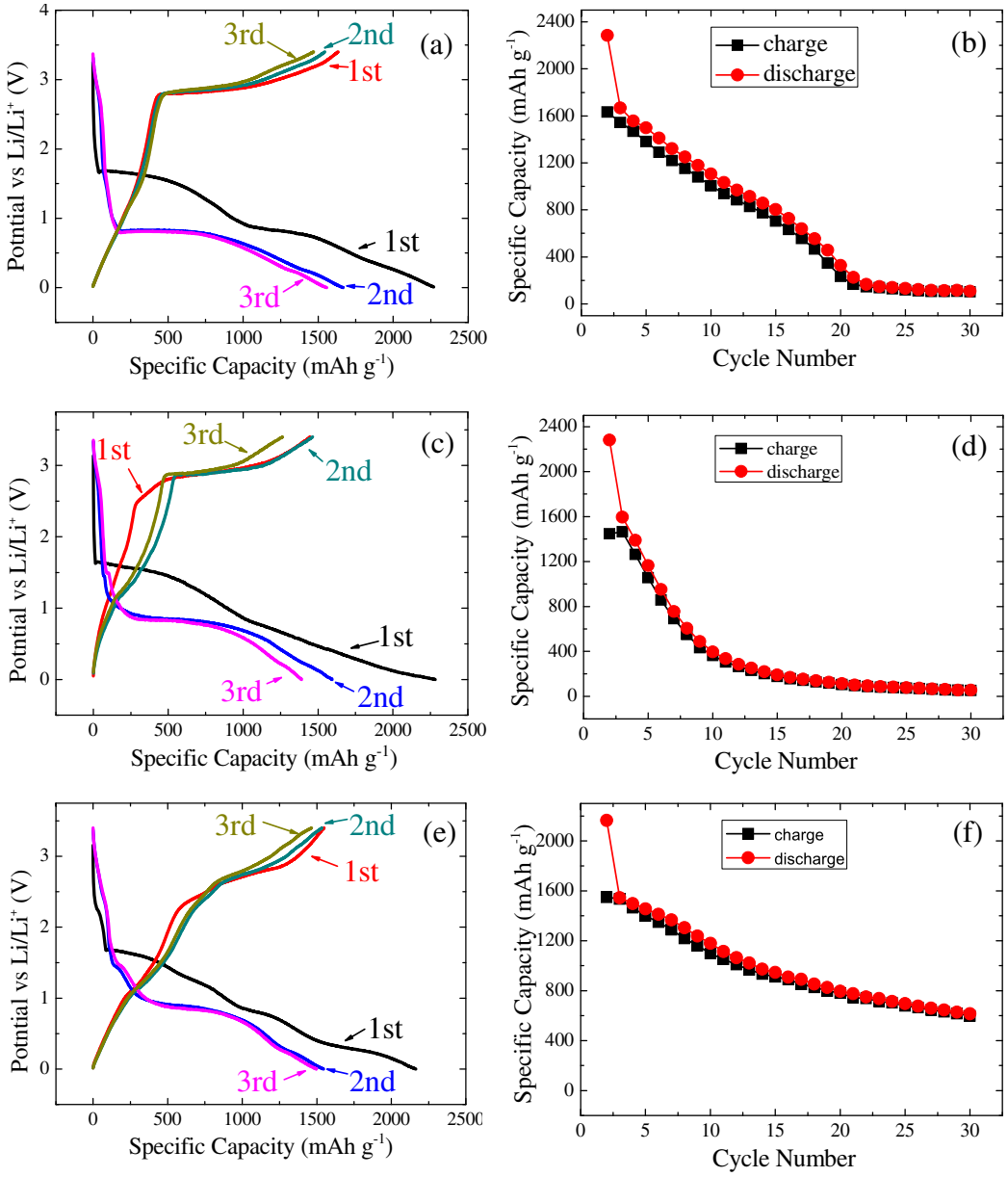

Fig. 3. Charge–discharge curves and corresponding cycling properties of $Cu(NO_3)_2{\cdot}xH_2O$ ($x \leq 2.5$) electrodes obtained at different heat-treatment temperatures. (a, b) 80 °C; (c, d) 120 °C; (e, f) 160 °C.

crystallized water contents of samples obtained at different heat-treatment temperatures. As shown in Fig. 3a, c and e, it can be observed that the first discharge capacities of $Cu(NO_3)_2{\cdot}xH_2O$ ($x \leq 2.5$) samples prepared at 80, 120 and 160 °C are 2269.5, 2282.2 and 2164.1 mAh g^{-1}, respectively. Obviously, the initial discharge capacity of $Cu(NO_3)_2{\cdot}xH_2O$($x \leq 2.5$)/Li cell is much higher than the original discharge capacity of CuO [18] or CuN [12]. However, the lithium storage capacities of $Cu(NO_3)_2{\cdot}xH_2O$ ($x \leq 2.5$) electrodes heat-treated at 80, 120 and 160 °C decrease sharply to the values of 1667.0, 1594.5 and 1545.2 mAh g^{-1} in the second discharge process, respectively. The decomposition of the electrolyte to form SEI film and the pulverization of active materials (as shown in Fig. 4) during conversion reaction process may be the main reasons for the irreversible capacity loss.

The cycling performance of $Cu(NO_3)_2{\cdot}xH_2O$ ($x \leq 2.5$) electrodes obtained at different heat-treatment temperatures are evaluated at a constant current density of 50 mA g^{-1} between 0.0 and 3.4 V and the electrochemical results are shown in Fig. 3b, d and f. It can be found that there are high initial reversible charge capacities reaching 1632.1, 1446.7 and 1549.3 mAh g^{-1} for $Cu(NO_3)_2{\cdot}xH_2O$ ($x \leq 2.5$) electrodes heat-treated at 80, 120 and 160 °C, respectively. The reversible specific capacity in the first discharge–charge process for $Cu(NO_3)_2{\cdot}xH_2O$ ($x \leq 2.5$) electrode is higher than the theoretical capacity of CuO (670 mAh g^{-1}). However, the capacity losses for $Cu(NO_3)_2{\cdot}xH_2O$ ($x \leq 2.5$) electrodes heat-treated at 80, 120 and 160 °C are 637.4, 835.5 and 596.8 mAh g^{-1}, respectively, due to the formation of SEI layer and the pulverization of active materials as shown in Fig. 4. Moreover, the reversible charge capacities of $Cu(NO_3)_2{\cdot}xH_2O$ ($x \leq 2.5$) electrodes heat-treated at 80 and 120 °C decrease sharply to the values of 102.8 and 52.5 mAh g^{-1} after 30 cycles, respectively, indicating poor cyclic performance as shown in Fig. 3b and d. The rapid deterioration of the reversible capacity is attributed to the huge volume changes during cycles. As a results, some $Cu(NO_3)_2{\cdot}xH_2O$ ($x \leq 2.5$) particles

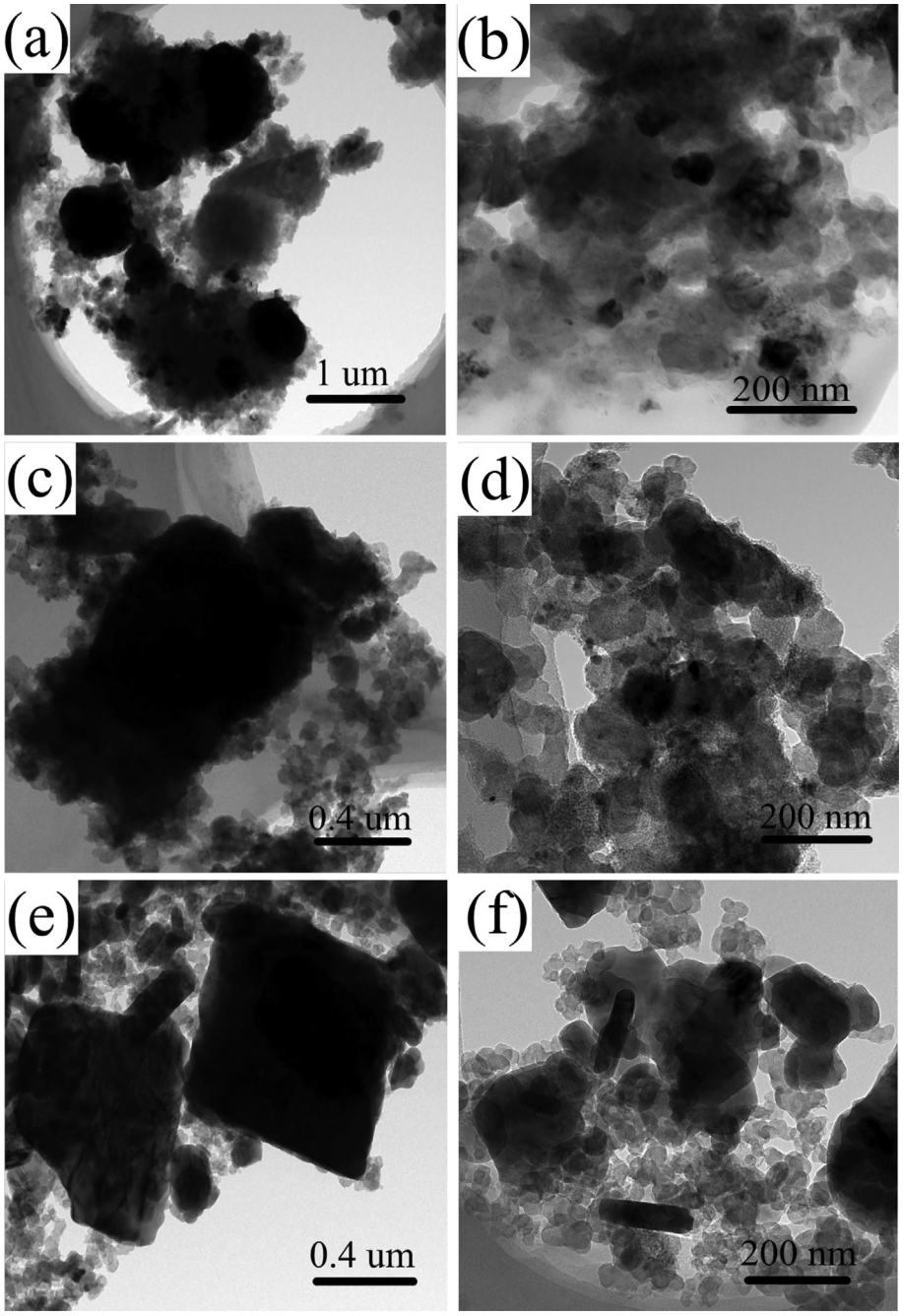

Fig. 4. SEM images of $Cu(NO_3)_2 \cdot xH_2O$ ($x \leq 2.5$) electrodes obtained at different heat-treatment temperatures before ((a) 80 °C; (c) 120 °C; (e) 160 °C) and after ((b) 80 °C; (d) 120 °C; (f) 160 °C) cycles.

lose electronic contacts and do not take part in the following cycles. For comparison, $Cu(NO_3)_2 \cdot xH_2O$ ($x < 2.5$) electrodes heat-treated at 160 °C show higher reversible capacity and better cycling capability as shown in Fig. 3f. After 30 cycles, a reversible capacity of 597.6 mAh g^{-1} can be delivered. The improved cycling performances can be ascribed to the homogeneous structure and highly dispersion particles obtained at 160 °C. Besides, owing to the change of surface morphology, the charge transfer resistance (R_{ct}) calculated from EIS pattern decreases from 200 Ω for sample heat-treated at 80 °C to 96 Ω for sample obtained at 160 °C as shown in Fig. 5. This result is consistent with the excellent calendar cycling life and high reversible specific capacity for $Cu(NO_3)_2 \cdot xH_2O$ ($x < 2.5$) electrode obtained at 160 °C as expressed in Fig. 3f. It suggests that the formed structure and surface morphology at 160 °C are beneficial to the migration of lithium ions and structural stability.

To study the thermal stability of lithiated $Cu(NO_3)_2 \cdot xH_2O$ ($x \leq 2.5$) samples, the TG-DTA curves are taken after the $Cu(NO_3)_2 \cdot xH_2O$($x \leq 2.5$)/Li cells were discharge to 0.0 V. Fig. 6a, b and c shows the thermal stabilities of lithiated $Cu(NO_3)_2 \cdot xH_2O$ ($x \leq 2.5$) materials obtained at 80, 120 and 160 °C, respectively. It is clear that the thermal reaction curves display similar behaviors with the rising of heat-treatment temperature. According to the thermal behaviors, it can be found that the decomposition process of lithiated samples displays four steps. As observed by the TG curve, there are four weight losses at 20–99 °C, 99–178 °C,

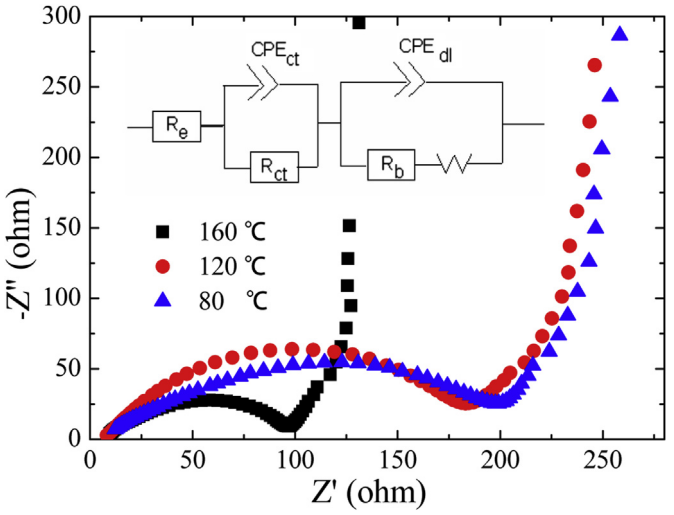

Fig. 5. Electrochemical impedance spectra and corresponding equivalent circuit of $Cu(NO_3)_2{\cdot}xH_2O$ ($x \leq 2.5$) electrodes obtained at different heat-treatment temperatures in a frequency range of 10^5–10^{-2} Hz.

178–320 °C and 320–600 °C, respectively. The observed weight loss of 4.74% at 20–99 °C may be attributed to the volatilization of electrolyte and water generated by the decomposition of $Cu(NO_3)_2{\cdot}xH_2O$ ($x \leq 2.5$) during discharging to 0.0 V. According to previous studies [19–21], the weight loss of 8.65% between 99 and 178 °C may be ascribed to the decomposition of SEI layers. Besides, the endothermic peak at around 150 °C are correlated to the decomposition of $ROCO_2Li$ into ROLi and CO_2 [22]. After that, the exothermic peak at 290.1 °C in the DTA curve, corresponding to the weight loss of 10.53% in 178–320 °C as deduced from the TG curve, may be due to the decomposition of ROLi and $LiPF_6$ and the formation of Li_2CO_3 and LiF [23]. Moreover, the weight loss of 5.46% between 320 and 600 °C in the TG curves should be attributed to the decomposition of final products generated after discharging to 0.0 V, such as $LiNO_3$. Compared with these results, it is obvious that $Cu(NO_3)_2{\cdot}xH_2O$ ($x < 2.5$) electrode obtained at 160 °C in Fig. 6c shows less total weight loss (13.6%) than that of the other two discharged samples, in which the total weight loss reaches to the values of 30.9% (80 °C) and 29.1% (120 °C) as shown in Fig. 6a and b. Moreover, the sample obtained at 160 °C shows much weaker endothermic and exothermic peaks than those appeared on the samples heat-treated at 80 and 120 °C. This result demonstrates that $Cu(NO_3)_2{\cdot}xH_2O$ ($x < 2.5$) electrode obtained at 160 °C has higher thermal stability than other two samples.

4. Conclusions

A novel nitrate compound, copper nitrate hydrate, is reported for the first time as a probable lithium storage candidate. The impressive characteristic of the $Cu(NO_3)_2{\cdot}xH_2O$($x \leq 2.5$)/Li cells over common graphite/Li cells may be the fact that the $Cu(NO_3)_2{\cdot}xH_2O$($x \leq 2.5$)/Li cells exhibit much higher initial discharge capacity of about 2200 mAh g^{-1} at a constant current density of 50 mA g^{-1}. The heat-treatment of $Cu(NO_3)_2{\cdot}2.5H_2O$ results in the variation of surface morphology, crystal water and particles size. It is clearly observed that $Cu(NO_3)_2{\cdot}xH_2O$ electrode obtained at 160 °C can deliver a higher reversible specific capacity of 597.6 mAh g^{-1} after 30 cycles than that of the samples heat-treated at 80 and 120 °C. Moreover, $Cu(NO_3)_2{\cdot}xH_2O$ ($x < 2.5$) electrode also show high thermal stability as a safe anode according to the thermal behaviors of lithiated samples. Therefore, $Cu(NO_3)_2{\cdot}xH_2O$ ($x < 2.5$) obtained at 160 °C exhibits its advantage and will be a suitable anode material for lithium-ion batteries.

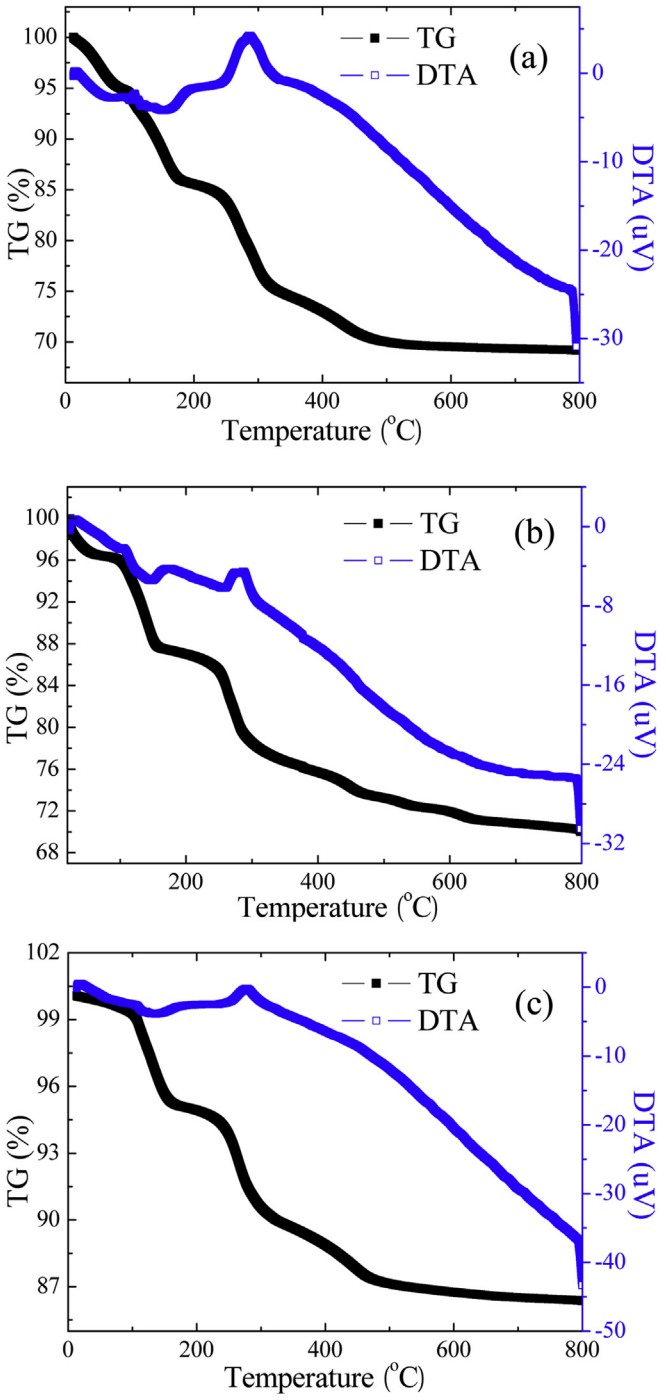

Fig. 6. TG-DTA curves of $Cu(NO_3)_2{\cdot}xH_2O$ ($x \leq 2.5$) electrodes obtained at different heat-treatment temperatures after a discharge process to 0.0 V. (a) 80 °C; (b) 120 °C; (c) 160 °C.

Acknowledgments

This work is sponsored by National 863 Program (2013AA050901) and National Natural Science Foundation of China (No. 51104092). The work is also supported by K.C. Wong Magna Fund in Ningbo University.

Appendix A. Supplementary data

Supplementary data related to this article can be found at http://dx.doi.org/10.1016/j.jpowsour.2013.09.079.

References

[1] A. Lamberti, M. Destro, S. Bianco, M. Quaglio, A. Chiodoni, C.F. Pirri, C. Gerbaldi, Electrochim. Acta 70 (2012) 62–68.
[2] J.Y. Xiang, J.P. Tu, X.H. Huang, Y.F. Yuan, X.L. Wang, X.H. Huang, Z.Y. Zeng, Electrochim. Acta 54 (2009) 1160–1165.
[3] J.Y. Xiang, J.P. Tu, X.H. Huang, Y.Z. Yang, J. Solid State Electrochem 8 (2008) 941–945.
[4] S.Q. Wang, J.Y. Zhang, C.H. Chen, Scr. Mater. 57 (2007) 337–340.
[5] M. Yang, Q.M. Gao, Microporous Mesoporous Mater. 143 (2011) 230–235.
[6] R. Stoyanova, E. Zhecheva, R. Alcantara, J.L. Tirado, G. Bromiley, F. Bromiley, T. Boffa Ballaran, Solid State Ionics 161 (2003) 197–204.
[7] Y.L. Ding, B.M. Goh, H. Zhang, K.P. Loh, L. Lu, J. Power Sources 236 (2013) 1–9.
[8] S.K. Chang, H.J. Kim, S.T. Hong, J. Power Sources 119–121 (2003) 69–75.
[9] Y.J. Mai, D. Zhang, Y.Q. Qiao, C.D. Gu, X.L. Wang, J.P. Tu, J. Power Sources 216 (2012) 201–207.
[10] M.Y. Li, Y. Wang, C.L. Liu, H. Gao, W.S. Dong, Electrochim. Acta 67 (2012) 187–193.
[11] Y.F. Wang, L.J. Zhang, J. Power Sources 209 (2012) 20–29.
[12] N. Pereira, L. Dupont, J.M. Tarascon, L.C. Llein, G.G. Amatucci, J. Electrochem. Soc. 149 (2002) A262–A271.
[13] N. Pereira, M. Balasubramanian, L. Dupont, J. Mcbreen, L.C. Klein, G.G. Amatucci, J. Electrochem. Soc. 150 (2003) A1118–A1128.
[14] Q. Sun, Z.W. Fu, Appl. Surf. Sci. 258 (2012) 3197–3201.
[15] M. Nishijima, Y. Takeda, N. Imanishi, O. Yamamoto, M. Takano, J. Solid State Chem. 113 (1994) 205–210.
[16] M. Nishijima, N. Tadokoro, Y. Takeda, N. Imanishi, O. Yamamoto, J. Electrochem. Soc. 141 (1994) 2966–2971.
[17] I.V. Morozov, K.O. Znamenkov, Yu.M. Korenev, O.A. Shlyakhtin, Electrochim. Acta 403 (2003) 173–179.
[18] J.Y. Xiang, J.P. Tu, L. Zhang, Y. Zhou, X.L. Wang, S.J. Shi, J. Power Sources 195 (2010) 313–319.
[19] H. Maleki, G. Deng, A. Anani, J. Electrochem. Soc. 146 (1999) 3224–3229.
[20] A. Du Pasquier, F. Disma, T. Bowmer, A.S. Gozdz, G. Amatucci, J.M. Tarascon, J. Electrochem. Soc. 145 (1998) 472–477.
[21] Y.S. Park, S.M. Lee, Electrochim. Acta 54 (2009) 3339–3343.
[22] M.H. Ryou, J.N. Lee, D.J. Lee, W.K. Kim, Y.K. Jeong, J.W. Choi, J.K. Park, Y.M. Lee, Electrochim. Acta 83 (2012) 259–263.
[23] Q.S. Wang, J.H. Sun, X.L. Yao, C.H. Chen, Thermochim. Acta 437 (2007) 12–16.